Helical dynamo growth at modest versus extreme magnetic Reynolds numbers

Hongzhe Zhou*
Tsung-Dao Lee Institute, Shanghai Jiao Tong University, 800 Dongchuan Road, Shanghai 200240, People's Republic of China and Nordita, KTH Royal Institute of Technology and Stockholm University, Hannes Alfvéns väg 12, SE-10691 Stockholm, Sweden

Eric G. Blackman†
Department of Physics and Astronomy, University of Rochester, Rochester, NY, 14627, USA and Laboratory for Laser Energetics, University of Rochester, Rochester NY, 14623, USA

(Dated: February 14, 2023)

How the growth of large-scale magnetic fields depends on microphysical transport has long been a focus of magnetic dynamo theory, and helical dynamo simulations have shown that the time to reach saturation in closed systems depends on the magnetic Reynolds number Rm. Because this would be too long for many high-Rm astrophysical systems, here we tackle the long-standing question of how much Rm-independent growth occurs earlier. From modest-Rm numerical simulations, we identify and explain a regime when the large-scale field grows independently of Rm, but to a magnitude that decreases with Rm. For plausible magnetic spectra however, the same analysis predicts the growth in this regime to be Rm−independent and provides a substantial lower bound for the field strength as $\mathrm{Rm}\to\infty$. The results provide renewed optimism for the relevance of closed dynamos and pinpoint how modest Rm and hyper-diffusive simulations can cause misapprehension of $\mathrm{Rm}\to\infty$ behavior.

Introduction.—The large-scale magnetic fields of many stars, planets, and galaxies require an *in situ* dynamo mechanism of sustenance against macroscopic or microscopic diffusion. Plausible dynamo models involve long-lived fields produced by collective motions of stochastic or turbulent eddies [1], often studied in the framework of mean-field electrodynamics [2]. In this approach, we look for solutions of a suitably averaged magnetic field that obeys the mean-field induction equation

$$\partial_t \overline{\boldsymbol{B}} = \boldsymbol{\nabla}\times\left(\overline{\boldsymbol{U}}\times\overline{\boldsymbol{B}}+\boldsymbol{\mathcal{E}}\right)+\eta\nabla^2\overline{\boldsymbol{B}}, \tag{1}$$

where $\boldsymbol{B}=\overline{\boldsymbol{B}}+\boldsymbol{b}$ is the total magnetic field measured in Alfvén units, $\overline{\cdot}$ is an average over a scale assumed to be much larger than the turbulent forcing scale (we use $\overline{\cdot}$ and $\langle\cdot\rangle$ interchangeably), and η is the magnetic diffusivity. We use lower case $\boldsymbol{b}$ to indicate the contribution to $\boldsymbol{B}$ with zero mean, and use similar constructions for the magnetic vector potential $\boldsymbol{A}$ and the velocity $\boldsymbol{U}$. For statistically homogeneous and isotropic, kinetically helical turbulence, the turbulent electromotive force (EMF) $\boldsymbol{\mathcal{E}}$ contains a term $\alpha\overline{\boldsymbol{B}}$ that is capable of amplifying $\overline{\boldsymbol{B}}$ [2–5]. Eventually the increasing Lorentz force back-reacts on the flow and quenches the dynamo.

A long-debated question is whether the quenching process becomes more severe at higher values of the magnetic Reynolds number Rm [6–13]. In the "dynamical quenching" (DQ) formalism, gradients of $\overline{\boldsymbol{B}}$ are required for it to grow, and the dynamo quenching is controlled by the conservation of magnetic helicity [14–19]. In this formalism, significant growth of the mean magnetic field occurs during an Rm-independent regime, after which Rm-dependent saturation occurs. In the nearly saturated stage, the field strength can reach super-equipartition values, but only on a resistively long time scale [17, 20, 21]. Although resistive time scales are appropriate for planets, the very large Rm in most astrophysical flows render the resistive growth time scale too long for stellar and galactic contexts. This in turn raises the important question of how strong the field gets before Rm dominates the evolution.

A substantial Rm-independent regime has not yet been concretely identified in previous numerical simulations. Hence, given the uncertainty of the Rm-dependence in the kinematic phase and the impractically long time scale for the fully saturated phase, it is a puzzle how astrophysical flows obtain appreciable field strengths from helical dynamo actions. Solutions to this problem include having helicity fluxes [e.g., 22–26] and using anisotropic forcing [27]. See Ref. [28] for a comprehensive review, and also Refs. [29–32] for reviews.

In this Letter, we investigate whether an Rm-independent regime might exist before the very long resistive phase. To be precise, we study the helical dynamo in a closed system during three distinct temporal stages: (i) a fast small-scale dynamo (SSD) that grows on turbulent time scales, (ii) a large-scale dynamo (LSD) that is $\mathcal{O}(10)$ times slower than the SSD, and (iii) a growth driven by magnetic helicity dissipation that operates on resistive time scales. At very early times when the magnetic energy is negligible to the kinetic energy at all scales, the SSD and LSD phases can be described in a unified framework [33–35]. Once the SSD comes to near saturation, LSD takes over and potentially operates independent of resistivity for some more extended time, sometimes termed a quasi-kinematic LSD [36, 37]. The

* hongzhe.zhou@sjtu.edu.cn
† blackman@pas.rochester.edu

resistive phase becomes dominant once the LSD saturates [17, 20, 38, 39]. Hence we ask, does the LSD phase amplify the mean field to some Rm-independent value before dynamical quenching transitions to the resistively limited asymptotic phase? We define the regime whose Rm dependence we wish to assess as the "pre-dynamically quenched" (PDQ) regime, a definition which will be made more precise later.

An unambiguous answer is challenging to obtain from numerical simulations without careful interpretation because of the poorly separated time scales of the LSD and the resistive phases given the moderate values of Rm available. Instead of using time to delineate dynamo phases, here we employ a new dynamo tracker which records how much the dynamo driver has been quenched. At each quenching level, we then analyze individually the Rm-dependence of the LSD growth rate, its time duration, and the field strength. We then discuss the distinct implications of our analysis for the modest Rm values obtainable in the simulations versus the implications for asymptotically large Rm.

Methods.—We perform compressible magnetohydrodynamics simulations with an isothermal equation of state using the Pencil Code [40, 41]. The velocity is driven in a $(2\pi)^3$-periodic box using positively helical plane waves at a fixed forcing wave number k_f, but with random phases and directions at each time step. The vector potential $\boldsymbol{A}$ is solved in the Weyl gauge, but periodic boundary conditions ensure that the magnetic helicity is gauge invariant. For all runs, we use $k_\mathrm{f} = 4$ and Mach numbers $\mathrm{Ma} \simeq 0.1$. The Reynolds numbers $\mathrm{Re} = u_\mathrm{rms}/\nu k_\mathrm{f}$ (with u_rms being the root-mean-square velocity and ν being the viscosity) are kept roughly constant, $\simeq 5$, and the magnetic Prandtl number $\mathrm{Pm} = \nu/\eta$ is varied from 1 to 100. This isolates the Rm dependence from the Re dependence.

We consider only the helical part of the magnetic field since that is most relevant to LSD dynamics. Although the current helicity spectrum $\mathcal{H}^\mathrm{C}$ is gauge-independent regardless of boundary conditions, it is more convenient here to formulate the equations using the magnetic helicity spectrum $\mathcal{H}^\mathrm{M}$. For the present boundary conditions, the two are simply related by $\mathcal{H}^\mathrm{C} = k^2\mathcal{H}^\mathrm{M}$ where k is the wave number. Throughout this work, energy and helicity spectra are normalized such that the integration over all the wave numbers yields the energy or helicity density. We then decompose the large- and small-scale magnetic helicity densities as

$$\int \mathcal{H}_i^\mathrm{M}\,\mathrm{d}k = s_i k_i^{-1} \int k \left|\mathcal{H}_i^\mathrm{M}\right|\,\mathrm{d}k, \tag{2}$$

where $i = 1, 2$ denote the large-scale ($k < k_\mathrm{f}$) and the small-scale ($k \geq k_\mathrm{f}$) modes, respectively, $s_i = \int \mathcal{H}_i^\mathrm{M}\,\mathrm{d}k / \int \left|\mathcal{H}_i^\mathrm{M}\right|\,\mathrm{d}k$ is the mean handedness, and $k_i = \int k \left|\mathcal{H}_i^\mathrm{M}\right|\,\mathrm{d}k / \int \left|\mathcal{H}_i^\mathrm{M}\right|\,\mathrm{d}k$ is the mean wave number. Note that $-1 \leq s_i \leq 1$ and $k_i > 0$. The non-dimensional energy density of the large-scale helical field is $\tilde{E}_\mathrm{L} = \int k|\mathcal{H}_1^\mathrm{M}|\,\mathrm{d}k/u_\mathrm{rms}^2$, where u_rms is the instantaneous root-mean-square (rms) value of the turbulent velocity. We define dimensionless time as $\tilde{t}(t) = \int_0^t u_\mathrm{rms}(t')k_\mathrm{f}\,\mathrm{d}t'$, which is monotonic in t, and reduces to $\tilde{t} = tu_\mathrm{rms}k_\mathrm{f}$ for constant u_rms. Hence $\tilde{t}$ roughly equals the number of turnovers of the largest eddies. We also define the dimensionless exponential growth rate $\tilde{\gamma} = \mathrm{d}\ln\tilde{E}_\mathrm{L}/\mathrm{d}\tilde{t}$.

Quenching mechanism.—We first demonstrate that DQ is the dominant quenching mechanism. For statistically isotropic and homogeneous turbulence, the turbulent EMF in Eq. (1) takes the form $\boldsymbol{\mathcal{E}} = \alpha\overline{\boldsymbol{B}} - \beta\boldsymbol{\nabla}\times\overline{\boldsymbol{B}}$. We write turbulent transport coefficients in general forms

$$\alpha = f(\tilde{E}_\mathrm{L}, \mathrm{Rm})\alpha_0 + \alpha_\mathrm{m}(\tilde{E}_\mathrm{L}, \mathrm{Rm}) \tag{3}$$

and

$$\beta = f(\tilde{E}_\mathrm{L}, \mathrm{Rm})\beta_0, \tag{4}$$

where the subscript 0 denotes the kinematic values, so α_0 is the kinetic contribution to α in the kinematic phase. We distinguish the magnetic feedback onto the velocity field itself, f, from that due to the helicity conservation constraint, α_m. The factor f captures the possible suppression of α_0 and turbulent diffusion β_0, as considered by Refs. [6–9], whereas α_m grows by DQ [14, 15, 17] and is related to the small-scale current helicity.

Without loss of generality, we consider the velocity field to be driven with positive kinetic helicity. In their isotropic forms [4, 14, 17],

$$\alpha_0 = -\frac{1}{3}\left\langle \tau_u \boldsymbol{u}\cdot\boldsymbol{\nabla}\times\boldsymbol{u}\right\rangle_0 \simeq -\frac{1}{3}\left(\int \frac{\mathcal{H}^\mathrm{K}}{k}\,\mathrm{d}k\right)_0^{1/2} \tag{5}$$

and

$$\alpha_\mathrm{m} = \frac{1}{3}\left\langle \tau_b \boldsymbol{b}\cdot\boldsymbol{\nabla}\times\boldsymbol{b}\right\rangle \simeq \frac{1}{3}\left(\int k^2\mathcal{H}_2^\mathrm{M}\,\mathrm{d}k\right)^{1/2}, \tag{6}$$

where $\mathcal{H}^\mathrm{K}$ is the kinetic helicity spectrum, and τ_u and τ_b are correlation times which are not necessarily equal. Similarly, $\beta_0 = \left(\tau_\beta u_\mathrm{rms}^2\right)_0/3$, and $\tau_\beta = 1/u_\mathrm{rms}k_\mathrm{f}$. We denote $\epsilon = \tau_u/\tau_\beta$ which is of order unity.

For a helical LSD without shear (i.e., an α^2 dynamo), the energy growth rate of a mode with wave number k_1 is $\gamma_\mathrm{LSD} = 2|\alpha|k_1 - 2(\beta+\eta)k_1^2$. Using Eqs. (3) and (4), the normalized growth rate is

$$\begin{aligned}\tilde{\gamma}_\mathrm{LSD} = \frac{\gamma_\mathrm{LSD}}{u_\mathrm{rms}k_\mathrm{f}} =& f\epsilon\frac{2u_\mathrm{rms,0}}{3u_\mathrm{rms}}\left(1-\chi\right)\frac{k_1}{k_\mathrm{f}} \\ &- \left(f\frac{2u_\mathrm{rms,0}}{3u_\mathrm{rms}} + \frac{2}{\mathrm{Rm}}\right)\left(\frac{k_1}{k_\mathrm{f}}\right)^2,\end{aligned} \tag{7}$$

where $\chi = -\alpha_\mathrm{m}/f\alpha_0$ is the DQ factor, $\mathrm{Rm} = u_\mathrm{rms}/\eta k_\mathrm{f}$ is the instantaneous magnetic Reynolds number, and we have considered a fully helical velocity field. To reveal the Rm dependence of f, we take $\epsilon = 1$ for the moment, as it does not change significantly with Rm in simulations. The f factor can then be calculated from Eq. (7), since all other quantities are measurable. The result is shown in

Fig. 1(a), and we see that f only weakly changes with $\tilde{E}_{\rm L}$ and Rm. Since both $\tilde{E}_{\rm L}$ and $\langle b^2 \rangle$ are nearly monotonic in time, this also implies that f is not strongly quenched by the small-scale field in three-dimensional systems. DQ is thus the dominant source of quenching and we can use χ to distinguish different dynamo phases.

As per Eq. (4), we absorb f into $\alpha_{\rm k} = f\alpha_0$, and therefore $\chi = -\alpha_{\rm m}/\alpha_{\rm k}$. Hence $\alpha = \alpha_{\rm k}(1-\chi)$, and

$$\tilde{\gamma}_{\rm LSD} = \epsilon \frac{2k_1}{3k_{\rm f}}(1-\chi) - \left(\frac{2}{3} + \frac{2}{\rm Rm}\right)\left(\frac{k_1}{k_{\rm f}}\right)^2. \quad (8)$$

Note that χ is roughly the normalized current helicity which manifests the Lorentz back-reaction of the LSD. The LSD initially operates kinematically when $\chi \ll 1$, but is then dynamically quenched by χ due to the growing small-scale current helicity. The maximal value χ can obtain is analytically determined by $\tilde{\gamma}_{\rm LSD} = 0$ to be roughly $1 - k_1/k_{\rm f}$ [18], which is $\leq 3/4$ in our cases. Resistive diffusion of magnetic helicity reduces the growth rate of χ, but does not directly show up in the LSD growth rate. We discuss its influence on LSD quenching later.

As χ grows from nearly 0 to $\simeq 3/4$, the value $\chi \simeq 0.1$ separates the SSD and LSD-dominated phases, as determined by two measurements: (i) The mean-to-rms ratio, $\overline{B}^2/B_{\rm rms}^2$, remains constant at $\chi \leq 0.1$ for all runs, which is a signature SSD feature. (ii) The SSD phase efficiently amplifies small-scale fields but with low fractional magnetic helicity, e.g. an average value of 0.05 for run A5. Thus values of $\chi > 0.1$ result from the LSD. The LSD regime for which $0.1 \leq \chi \leq 0.6$ quantitatively demarks the PDQ regime whose Rm dependence we will assess.

In our simulations, χ is nearly monotonic in time with some fluctuations. In what follows, any quantity taken at $\chi = \chi'$ is meant to be its average over the interval $\chi \in [\chi' - \delta', \chi' + \delta]$ with $\delta = \min\{0.2\chi', 0.05\}$, unless otherwise specified.

Rm-dependence of LSD.—We first compare Eq. (8) with numerical results. We rearrange this equation to

$$\sigma = \frac{3k_{\rm f}}{2k_1}\tilde{\gamma} + \left(1 + \frac{3}{\rm Rm}\right)\frac{k_1}{k_{\rm f}}, \quad (9)$$

where $\sigma = \epsilon(1-\chi)$, and for some given χ, we expect σ to depend on Rm at most weakly through ϵ. Fig. 1(b) shows our simulation values of σ as a function of χ, with varying Rm for different curves. The observation that σ becomes Rm-independent once Rm $\gtrsim 130$, together with Eq. (9) and the fact that k_1 is bounded from below, implies that $\tilde{\gamma}$ is independent of Rm as Rm $\to \infty$. An Rm-independent growth rate was previously reported [37] at Rm $\gtrsim 500$, but here we provide evidence at lower Rm.

Overall, the measured values of σ are lower than $(1-\chi)$, and $\epsilon = 0.8$ is sufficient to explain the deviation, as indicated by the two black dashed lines in Fig. 1(b). This time scale difference in the $\alpha_{\rm k}$ and β coefficients might explain the lower-than-unity LSD efficiency previously reported by Ref. [37].

We next examine the normalized duration $\Delta\tilde{t}(\chi_{\rm i}, \chi_{\rm f})$ that the LSD spends in the interval $\chi_{\rm i} \leq \chi \leq \chi_{\rm f}$. This is plotted in Fig. 2 for a number of pairs of $(\chi_{\rm i}, \chi_{\rm f})$. The results show no significant scaling with Rm. Hence, the e-folding of the LSD for a given range of χ, namely the product of the normalized LSD growth rate and growth duration, is asymptotically independent of Rm.

However, the non-dimensional large-scale helical field energy density, $\tilde{E}_{\rm L}(\chi, {\rm Rm})$, does decrease with increasing Rm at fixed χ, although the ratio $\tilde{E}_{\rm L}(\chi_{\rm f}, {\rm Rm})/\tilde{E}_{\rm L}(\chi_{\rm i}, {\rm Rm})$ is weakly sensitive to Rm. To see how $\tilde{E}_{\rm L}(\chi, {\rm Rm})$ depends on Rm, we define a scaling exponent p by fitting a power-law relation $\tilde{E}_{\rm L}(\chi, {\rm Rm}) \propto {\rm Rm}^{p(\chi)}$, as shown in Fig. 3. We see that p is consistently negative for all χ, indicating that at all stages of the LSD, the mean-field energy decreases with increasing Rm. We next explain this dependence for the simulations and discuss what happens at asymptotically much larger Rm, and the modest Rm simulation may disguise an Rm-independence as Rm $\to \infty$.

Understanding the relation between $\tilde{E}_L$ and Rm—The large-scale field strength decreases with increasing Rm at a fixed χ, but for different reasons in the SSD and LSD phases. In the SSD phase at $\chi \simeq 0.01$, the negative scaling $\tilde{E}_{\rm L} \propto {\rm Rm}^{-0.5}$ for our Pm ≥ 1 cases is similar to the result of Refs. [35, 42] that $\overline{B}/B_{\rm rms} \propto {\rm Rm}^{-3/4}$ for Pm $= 0.1$ cases. In fact, we find that the ratio $\overline{B}/B_{\rm rms}$ is a constant at $\chi \leq 0.1$ for each run (roughly 300 eddy turnover times), but is $\propto {\rm Rm}^{-1/2}$. That $\overline{B}$ and $B_{\rm rms}$ grow at the same rate is a signature of the SSD phase (or, in the language of Ref. [35], a feature of the kinematic, not quasi-kinematic, dynamo phase), although the origin of $-1/2$ is not yet fully understood [42].

In the LSD phase for $\chi \geq 0.1$, $\tilde{E}_{\rm L}$ can be inferred from the total magnetic helicity without integrating the growth equation. Consider the case where the volume-averaged magnetic helicity is zero initially, but later gains $\Delta H = H_1^{\rm M} + H_2^{\rm M}$ due to resistive diffusion, where $H_{1,2}^{\rm M}$ are the average magnetic helicity of the large- and small-scale fields, respectively. Using Eq. (2) we have $H_1^{\rm M} = s_1 k_1^{-1} \tilde{E}_{\rm L} u_{\rm rms}^2$, and

$$\tilde{E}_{\rm L}(\chi, {\rm Rm}) = -\frac{k_1}{s_1}\frac{H_2^{\rm M}}{u_{\rm rms}^2} + \frac{k_1 \Delta H}{s_1 u_{\rm rms}^2}. \quad (10)$$

We denote the two terms on the right of Eq. (10) by T_1 and T_2, so that $\tilde{E}_{\rm L} = T_1 + T_2$. Note that T_2 is from the resistive loss of magnetic helicity but T_1 is purely dynamic, so that the magnitude of their ratio determines whether resistive effects dominate and this is to be assessed below.

For all runs at all times, the magnetic fields near the resistive wave number have positive magnetic helicity, whilst those at the lowest wave numbers have negative helicity. Hence $\Delta H < 0$ and $s_1 < 0$ always. However, as we will see shortly, $H_2^{\rm M}$ may have the same sign as s_1 at early times, so then T_1 can be negative.

The evolution of $T_{1,2}/\tilde{E}_{\rm L}$, is shown in Fig. 4. For the three runs with the highest Rm, we see $T_1/\tilde{E}_{\rm L} < 0$ and

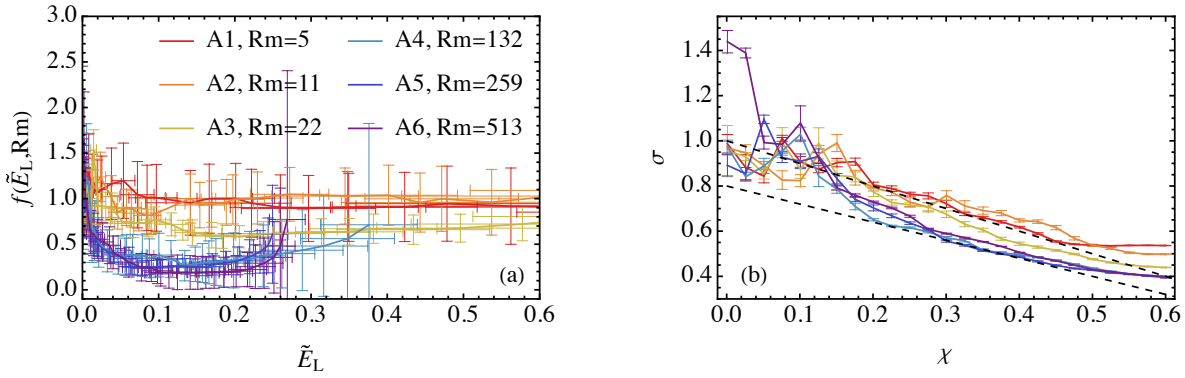

FIG. 1. The Rm dependence of the runs. (a) The quenching factor f versus the dimensionless large-scale helical magnetic energy $\tilde{E}_{\rm L}$. (b) The measured values of σ [Eq. (9)], as a function of χ with different Rm. The two black dashed lines indicate the theoretical values $\epsilon(1-\chi)$ with $\epsilon = 1$ (upper) and $\epsilon = 0.8$ (lower).

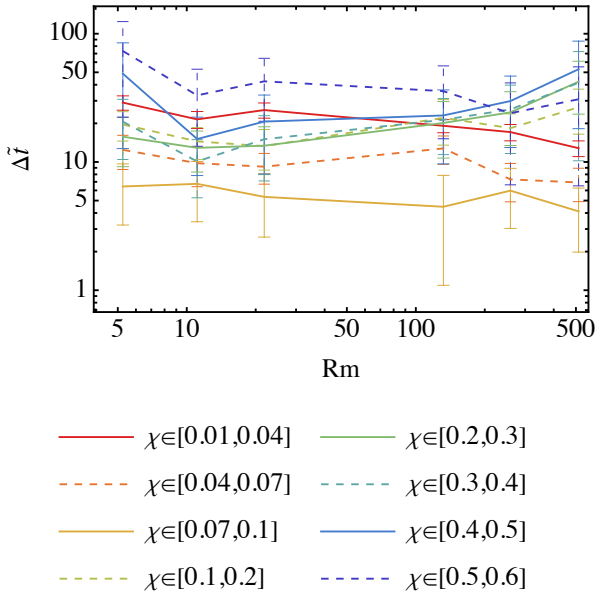

FIG. 2. The time duration in each $\chi_{\rm i} \le \chi \le \chi_{\rm f}$ intervals.

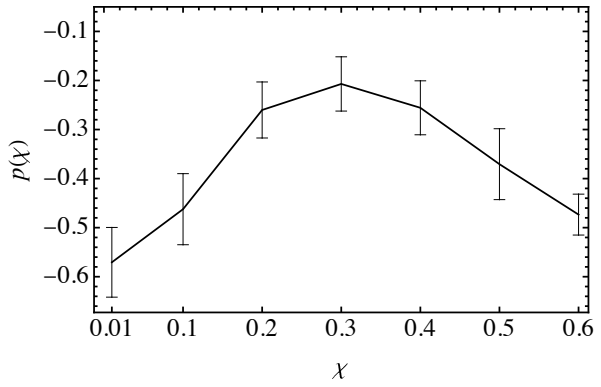

FIG. 3. The power index p in $\tilde{E}_{\rm L}(\chi) \propto {\rm Rm}^p$ for each χ, by fitting all the runs in group A.

$T_2/\tilde{E}_{\rm L} > 1$ during the SSD phase. That $T_1 < 0$ and $s_1 < 0$ implies a negative average handedness of the small-scale field, $s_2 < 0$ [see Eq. (2)]. This is because at that time, negative helicity resides on a wide range of k, particularly at both $k < k_{\rm f}$ and a finite range at $k \ge k_{\rm f}$. This implies that, since the field at k_1 is already fully helical, $k_1 \Delta H/s_1$ alone would overestimate the large-scale contribution, i.e., $T_2/\tilde{E}_{\rm L} > 1$.

In fact, the initial dividing wave number $k_{\rm div}$ between the positively and negatively helical parts is not $k_{\rm f}$, but roughly the viscous wave number k_ν. The SSD initially operates most efficiently on the viscous scale, and generates positively helical fields at $k > k_\nu$. Conservation of magnetic helicity requires that negatively signed magnetic helicity must compensate at $k < k_\nu$ at a generation rate comparable to that of the efficient SSD at k_ν. Thus, the net sign of helicity at $k < k_\nu$ is initially negative. As the SSD at k_ν approaches saturation, its back-reaction that produces negative helicity on larger scales eventually becomes slower than the SSD rate below k_ν, and so positive helicity starts to build up there and we see $k_{\rm div}$ decreasing, until eventually it reaches $k_{\rm div} = k_{\rm f}$. Hence, $s_2 < 0$ during the kinematic SSD phase but becomes positive when the SSD saturates. For this reason, at early times, Eq. (10) can be interpreted as conservation of magnetic helicity during SSD, before the LSD is influential.

The LSD starts to dominate the field growth at k_1 at $\chi \gtrsim 0.1$, and its back-reaction on the small scales grows T_1. Note that in the LSD-dominated regime, s_1 has the same sign as ΔH and the opposite sign to $H_2^{\rm M}$, so that $T_{1,2} > 0$ always. By the time $\chi = 0.6$ which is close to the end of the LSD regime, Eq. (10) determines how much the LSD has benefitted from resistive contributions. That $T_1 < T_2$ implies that the LSD quenching is still weakened substantially by the resistive dissipation of small-scale current helicity, and therefore the PDQ regime depends strongly on Rm. This is why $p < 0$ at $\chi \ge 0.1$ [Fig. 3]. Note that the resistive term does not amplify the large-scale field directly, but slows the growth of χ, thereby weakening the back-reaction and allowing

more large-scale growth of $\tilde{E}_{\rm L}(\chi)$.

Implications for higher Rm.—From Fig. 4 we see that by $\chi = 0.6$, the contribution from T_1 increases and that from T_2 decreases with increasing Rm. However, for the highest Rm runs A5 and A6, the ratio T_2/T_1 has reached saturation and no longer decreases with increasing Rm. This could be because the LSD has not fully saturated at $\chi \simeq 0.6$, or because T_2/T_1 is not monotonic in Rm. Regardless, it is interesting to assess whether T_1 might dominate before the resistive phase in the large Rm regime, and/or become independent of Rm. Since $T_2 \propto \Delta H$ and becomes negligibly small during the LSD phase in the Rm $\to \infty$ limit, the necessary condition for Rm-independent PDQ regime is that $\mathrm{d}|T_1|/\mathrm{dRm} \to 0$ as Rm $\to \infty$. In the LSD phase, $\mathcal{H}_2^{\rm M}$ is of one sign, so we can write $T_1 = -s_2 k_1 \chi^2 / s_1 k_2$. Since $|s_{1,2}| \simeq 1$, and k_1 is bounded from below, Rm-independent PDQ regime requires k_2 to depend at most weakly on Rm at fixed χ, which will be fully determined by the helicity spectrum.

Consider a power-law magnetic helicity spectrum, $\mathcal{H}^{\rm M}(k) \propto k^{-q}$, in the inertial range. This is appropriate for Pm < 1 flows. Using Eq. (2) for k_2, we then have that $k_{\rm f}/k_2 = F(q)/F(q-1)$, where $F(q) = \int_1^r x^{-q}\,\mathrm{d}x$, $r = k_{\rm dis}/k_{\rm f}$, and $k_{\rm dis}$ is the dissipation wave number of the helical fields that might be different from the resistive scale. In any case, $r \gg 1$ when Rm $\to \infty$. In that Rm $\to \infty$ limit,

$$\frac{k_{\rm f}}{k_2} \to \begin{cases} \dfrac{q-2}{q-1}, & q > 2, \\ \dfrac{1}{\ln r}, & q = 2, \\ \dfrac{2-q}{q-1}\dfrac{1}{r^{2-q}}, & 1 < q < 2, \\ \dfrac{\ln r}{r}, & q = 1, \\ \dfrac{2-q}{1-q}\dfrac{1}{r}, & q < 1 \end{cases}. \tag{11}$$

Hence Rm-independent PDQ regime happens if $q > 2$, i.e., the magnetic helicity spectrum is sufficiently steep.

For Pm > 1 flows whose magnetic energy and helicity spectra may have broken power laws at $k \geq k_{\rm f}$, the conditions for an Rm-independent PDQ regime become (i) a $q > 2$ range exists, and (ii) the wave number above which $q > 2$ does not increase with increasing Rm. From our Pm ≥ 1 simulations, we observe spectral slopes $q < 2$ at $k_{\rm f} < k < 2k_{\rm f}$ and $q > 2$ at $k > 2k_{\rm f}$ for runs A5 and A6 at $\chi = 0.6$. Hence the PDQ regime would be Rm-independent as Rm $\to \infty$ if the wave number at which $q - 2$ changes sign ($\simeq 2k_{\rm f}$ here) is Rm-independent, as seen for runs A5 and A6 (Rm $\simeq 250$ and 500). This is consistent with previous indications that the peak wave number of the magnetic energy spectrum for large-Pm SSDs remains Rm-independent for large Rm from both theory [33] and simulation [43].

The spectrum may also evolve from shallower than the aforementioned threshold at early times to steeper at later times. Then the influence of Rm on the saturated state could still be small, as is crudely suggested in a four-scale approach [18]. Future high-resolution simulations for both Pm > 1 and Pm < 1 are needed to concretely confirm the spectral slope of the magnetic helicity at large Rm and its temporal evolution.

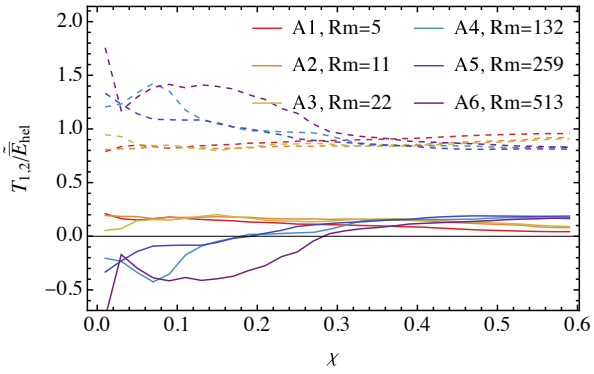

FIG. 4. $T_1/\tilde{E}_{\rm L}$ in solid and $T_2/\tilde{E}_{\rm L}$ in dashed curves.

To summarize, for a magnetic helicity spectrum that satisfies the conditions mentioned above, the Rm-independent value that $\tilde{E}_{\rm L}$ can obtain at any χ is

$$\lim_{\rm Rm\to\infty} \tilde{E}_{\rm L}(\chi, \mathrm{Rm}) = \lim_{\rm Rm\to\infty} T_1 = -\frac{s_2}{s_1}\frac{k_1}{k_{\rm peak}}\frac{q-2}{q-1}\chi^2, \tag{12}$$

where $k_{\rm peak}$ is the Rm-independent peak of the magnetic helicity spectrum. Eq. (12) is the lower bound for any case with a finite Rm (for which $T_2 > 0$), and indeed for all of our simulation runs, we observe $\tilde{E}_{\rm L}/(\chi^2 k_1/k_{\rm f})$ is ≥ 2.5, again highlighting the dominance of the resistive contribution for these runs.

Conclusions.—Focusing on the previously sparsely studied, but important, regime of LSD growth after the SSD saturates but before the LSD does, we arrive at three distinct results: (i) For isotropically helically forced flows, our simulations and theoretical analyses reveal that the large-scale field growth rate becomes Rm-independent at modest Rm and agrees well with the DQ formalism. Namely, the kinetic part to α remains Rm-independent during the course of the simulation and the Lorentz-force back-reaction that ends the LSD regime exerts itself not by suppressing $\alpha_{\rm k}$ but by growth of $\alpha_{\rm m}$. (ii) In contrast, the large-scale field strength attained in this PDQ regime for Rm values accessible in simulations is Rm-dependent, being dominated by the resistive loss of magnetic helicity even for Rm $\simeq 500$. (iii) However, the same theoretical analysis of the LSD shows that the Rm $\to \infty$ dependence of this PDQ regime depends on the evolution of the current helicity spectrum, or equivalently the magnetic helicity spectrum given the present boundary conditions. For sufficiently steep magnetic helicity spectra, the analysis shows that the regime becomes Rm-independent at asymptotically large Rm, with the large-scale magnetic energy lower bound given by Eq. (12).

Taken at face value, these results imply that when

the current helicity spectrum falls off more steeply than k^0, high-Rm flows in stars and galaxies that involve an α^2 or α^2-Ω effect could be capable of efficient LSD field growth even without boundary helicity fluxes, although systems requiring fast cycle periods would favor helicity flux driven dynamos. For shallower spectra, helicity fluxes or some non-helically driven LSD [e.g. 44] would be necessary even to explain the observed field strengths, let alone fast cycle periods. For planetary dynamos whose resistive time scales can be comparable to LSD dynamical time scales, α quenching is significantly weakened by resistive diffusion and therefore the LSD is much less constrained by the slope of the current helicity spectrum.

Finally, hyper-diffusivity is sometimes used for mimicking high-Rm flows [20]. Because the dissipation rate depends strongly on wave number, magnetic energy piles up near the resistive scale (bottleneck effect) [45]. If these resistive scale fields are helical, k_2 becomes large and our analysis shows that the quasi-kinematic LSD phase is strongly quenched even though it eventually leads to super-equipartition magnetic energies. Hence, helical LSDs with hyper-diffusion are actually less effective for inferring realistic asymptotic behaviors of LSDs.

Nordita is sponsored by Nordforsk. We acknowledge the allocation of computing resources provided by the Swedish National Allocations Committee at the Center for Parallel Computers at the Royal Institute of Technology in Stockholm and Linköping. EB acknowledges the Isaac Newton Institute for Mathematical Sciences, Cambridge, for support and hospitality during the programme "Frontiers in dynamo theory: from the Earth to the stars" where some work on this paper was undertaken. This work was supported by EPSRC grant no EP/R014604/1. EB acknowledges support from grants US Department of Energy DE-SC0001063, DE-SC0020432, DE-SC0020103, and US NSF grants AST-1813298, PHY-2020249.

The data and post-processing programs for this article are available on Zenodo at doi:10.5281/zenodo.7632994 [41].

[1] E. N. Parker, Hydromagnetic Dynamo Models., ApJ **122**, 293 (1955).

[2] M. Steenbeck, F. Krause, and K. H. Rädler, Berechnung der mittleren LORENTZ-Feldstärke für ein elektrisch leitendes Medium in turbulenter, durch CORIOLIS-Kräfte beeinflußter Bewegung, Zeitschrift Naturforschung Teil A **21**, 369 (1966).

[3] H. K. Moffatt, *Magnetic field generation in electrically conducting fluids* (Cambridge University Press, 1978).

[4] K.-H. Rädler, N. Kleeorin, and I. Rogachevskii, The Mean Electromotive Force for MHD Turbulence: The Case of a Weak Mean Magnetic Field and Slow Rotation, Geophysical and Astrophysical Fluid Dynamics **97**, 249 (2003), arXiv:astro-ph/0209287 [astro-ph].

[5] K.-H. Rädler and R. Stepanov, Mean electromotive force due to turbulence of a conducting fluid in the presence of mean flow, Physical Review E **73**, 056311 (2006), arXiv:physics/0512120 [physics.flu-dyn].

[6] R. M. Kulsrud and S. W. Anderson, The Spectrum of Random Magnetic Fields in the Mean Field Dynamo Theory of the Galactic Magnetic Field, ApJ **396**, 606 (1992).

[7] F. Cattaneo and S. I. Vainshtein, Suppression of Turbulent Transport by a Weak Magnetic Field, ApJL **376**, L21 (1991).

[8] S. I. Vainshtein and F. Cattaneo, Nonlinear Restrictions on Dynamo Action, ApJ **393**, 165 (1992).

[9] A. V. Gruzinov and P. H. Diamond, Self-consistent theory of mean-field electrodynamics, Phys. Rev. Lett. **72**, 1651 (1994).

[10] A. V. Gruzinov and P. H. Diamond, Self-consistent mean field electrodynamics of turbulent dynamos, Physics of Plasmas **2**, 1941 (1995).

[11] A. V. Gruzinov and P. H. Diamond, Nonlinear mean field electrodynamics of turbulent dynamos, Physics of Plasmas **3**, 1853 (1996).

[12] M. Ossendrijver, M. Stix, and A. Brandenburg, Magnetoconvection and dynamo coefficients:. Dependence of the alpha effect on rotation and magnetic field, A&A **376**, 713 (2001), arXiv:astro-ph/0108274 [astro-ph].

[13] S. M. Tobias and F. Cattaneo, Shear-driven dynamo waves at high magnetic Reynolds number, Nature **497**, 463 (2013).

[14] A. Pouquet, U. Frisch, and J. Leorat, Strong MHD helical turbulence and the nonlinear dynamo effect, Journal of Fluid Mechanics **77**, 321 (1976).

[15] N. Kleeorin and A. Ruzmaikin, Dynamics of the average turbulent helicity in a magnetic field, Magnetohydrodynamics **18**, 116 (1982).

[16] E. G. Blackman and G. B. Field, Constraints on the Magnitude of α in Dynamo Theory, ApJ **534**, 984 (2000), arXiv:astro-ph/9903384 [astro-ph].

[17] E. G. Blackman and G. B. Field, New Dynamical Mean-Field Dynamo Theory and Closure Approach, Phys. Rev. Lett. **89**, 265007 (2002), arXiv:astro-ph/0207435 [astro-ph].

[18] E. G. Blackman, Understanding helical magnetic dynamo spectra with a non-linear four-scale theory, MNRAS **344**, 707 (2003), arXiv:astro-ph/0301432 [astro-ph].

[19] A. Brandenburg, K.-H. Rädler, M. Rheinhardt, and K. Subramanian, Magnetic Quenching of α and Diffusivity Tensors in Helical Turbulence, ApJL **687**, L49 (2008), arXiv:0805.1287 [astro-ph].

[20] A. Brandenburg and G. R. Sarson, Effect of Hyperdiffusivity on Turbulent Dynamos with Helicity, Phys. Rev. Lett. **88**, 055003 (2002), arXiv:astro-ph/0110171 [astro-ph].

[21] S. Candelaresi and A. Brandenburg, Kinetic helicity needed to drive large-scale dynamos, Physical Review E **87**, 043104 (2013), arXiv:1208.4529 [astro-ph.SR].

[22] E. T. Vishniac and J. Cho, Magnetic Helicity Conservation and Astrophysical Dynamos, ApJ **550**, 752 (2001), arXiv:astro-ph/0010373 [astro-ph].

[23] K. Subramanian and A. Brandenburg, Nonlinear Current Helicity Fluxes in Turbulent Dynamos and Alpha Quenching, Phys. Rev. Lett. **93**, 205001 (2004), arXiv:astro-ph/0408020 [astro-ph].

[24] A. Hubbard and A. Brandenburg, Catastrophic Quenching in $\alpha\Omega$ Dynamos Revisited, ApJ **748**, 51 (2012), arXiv:1107.0238 [astro-ph.SR].

[25] F. Rincon, Helical turbulent nonlinear dynamo at large magnetic Reynolds numbers, Physical Review Fluids **6**, L121701 (2021), arXiv:2108.12037 [physics.flu-dyn].

[26] K. Gopalakrishnan and K. Subramanian, Magnetic helicity fluxes from triple correlators, arXiv e-prints , arXiv:2209.14810 (2022), arXiv:2209.14810 [astro-ph.GA].

[27] P. Bhat, Saturation of large-scale dynamo in anisotropically forced turbulence, MNRAS **509**, 2249 (2022), arXiv:2108.08740 [astro-ph.SR].

[28] A. Brandenburg and K. Subramanian, Astrophysical magnetic fields and nonlinear dynamo theory, Physics Reports **417**, 1 (2005), arXiv:astro-ph/0405052 [astro-ph].

[29] A. Brandenburg, Advances in mean-field dynamo theory and applications to astrophysical turbulence, Journal of Plasma Physics **84**, 735840404 (2018), arXiv:1801.05384 [physics.flu-dyn].

[30] D. W. Hughes, Mean field electrodynamics: triumphs and tribulations, Journal of Plasma Physics **84**, 735840407 (2018), arXiv:1804.02877 [astro-ph.SR].

[31] F. Rincon, Dynamo theories, Journal of Plasma Physics **85**, 205850401 (2019), arXiv:1903.07829 [physics.plasm-ph].

[32] A. Brandenburg and E. Ntormousi, Galactic Dynamos, arXiv e-prints , arXiv:2211.03476 (2022), arXiv:2211.03476 [astro-ph.GA].

[33] K. Subramanian, Unified Treatment of Small- and Large-Scale Dynamos in Helical Turbulence, Phys. Rev. Lett. **83**, 2957 (1999), arXiv:astro-ph/9908280 [astro-ph].

[34] S. Boldyrev, F. Cattaneo, and R. Rosner, Magnetic-Field Generation in Helical Turbulence, Phys. Rev. Lett. **95**, 255001 (2005), arXiv:astro-ph/0504588 [astro-ph].

[35] P. Bhat, K. Subramanian, and A. Brandenburg, A unified large/small-scale dynamo in helical turbulence, MNRAS **461**, 240 (2016), arXiv:1508.02706 [astro-ph.GA].

[36] J. Pietarila Graham, E. G. Blackman, P. D. Mininni, and A. Pouquet, Not much helicity is needed to drive large-scale dynamos, Physical Review E **85**, 066406 (2012), arXiv:1108.3039 [physics.flu-dyn].

[37] P. Bhat, K. Subramanian, and A. Brandenburg, Efficient quasi-kinematic large-scale dynamo as the small-scale dynamo saturates, arXiv e-prints , arXiv:1905.08278 (2019), arXiv:1905.08278 [astro-ph.GA].

[38] A. Brandenburg, The Inverse Cascade and Nonlinear Alpha-Effect in Simulations of Isotropic Helical Hydromagnetic Turbulence, ApJ **550**, 824 (2001), arXiv:astro-ph/0006186 [astro-ph].

[39] G. Bermudez and A. Alexakis, Saturation of Turbulent Helical Dynamos, Phys. Rev. Lett. **129**, 195101 (2022), arXiv:2204.14091 [physics.flu-dyn].

[40] Pencil Code Collaboration, A. Brandenburg, A. Johansen, P. Bourdin, W. Dobler, W. Lyra, M. Rheinhardt, S. Bingert, N. Haugen, A. Mee, F. Gent, N. Babkovskaia, C.-C. Yang, T. Heinemann, B. Dintrans, D. Mitra, S. Candelaresi, J. Warnecke, P. Käpylä, A. Schreiber, P. Chatterjee, M. Käpylä, X.-Y. Li, J. Krüger, J. Aarnes, G. Sarson, J. Oishi, J. Schober, R. Plasson, C. Sandin, E. Karchniwy, L. Rodrigues, A. Hubbard, G. Guerrero, A. Snodin, I. Losada, J. Pekkilä, and C. Qian, The Pencil Code, a modular MPI code for partial differential equations and particles: multipurpose and multiuser-maintained, The Journal of Open Source Software **6**, 2807 (2021), arXiv:2009.08231 [astro-ph.IM].

[41] H. Zhou and E. Blackman, Dataset for "Helical dynamo growth at modest versus extreme magnetic Reynolds numbers", 10.5281/zenodo.7632994 (2023), Zenodo.

[42] K. Subramanian and A. Brandenburg, Traces of large-scale dynamo action in the kinematic stage, MNRAS **445**, 2930 (2014), arXiv:1408.4416 [astro-ph.GA].

[43] A. K. Galishnikova, M. W. Kunz, and A. A. Schekochihin, Tearing Instability and Current-Sheet Disruption in the Turbulent Dynamo, Physical Review X **12**, 041027 (2022), arXiv:2201.07757 [astro-ph.HE].

[44] V. Skoutnev, J. Squire, and A. Bhattacharjee, On large-scale dynamos with stable stratification and the application to stellar radiative zones, MNRAS **517**, 526 (2022), arXiv:2203.01943 [astro-ph.SR].

[45] D. Biskamp, E. Schwarz, and A. Celani, Nonlocal Bottleneck Effect in Two-Dimensional Turbulence, Phys. Rev. Lett. **81**, 4855 (1998), arXiv:chao-dyn/9807012 [nlin.CD].